Selected Reaction Monitoring to Differentiate and Relatively Quantitate Isomers of Sulfated and Unsulfated Core 1 *O*-Glycans from Salivary MUC7 Protein in Rheumatoid Arthritis*

Sarah A. Flowers‡, Liaqat Ali‡, Catherine S. Lane§, Magnus Olin¶, and Niclas G. Karlsson‡‖

Rheumatoid arthritis is a common and debilitating systemic inflammatory condition affecting up to 1% of the world's population. This study aimed to investigate the immunological significance of *O*-glycans in chronic arthritis at a local and systemic level. *O*-Glycans released from synovial glycoproteins during acute and chronic arthritic conditions were compared and immune-reactive glycans identified. The sulfated core 1 *O*-glycan (Galβ1–3GalNAcol) was immune reactive, showing a different isomeric profile in the two conditions. From acute reactive arthritis, three isomers could be sequenced, but in patients with chronic rheumatoid arthritis, only a single 3-Gal sulfate-linked isomer could be identified. The systemic significance of this glycan epitope was investigated using the salivary mucin MUC7 in patients with rheumatoid arthritis and normal controls. To analyze this low abundance glycan, a selected reaction monitoring (SRM) method was developed to differentiate and relatively quantitate the core 1 *O*-glycan and the sulfated core 1 *O*-glycan Gal- and GalNAc-linked isomers. The acquisition of highly sensitive full scan linear ion trap MS/MS spectra in addition to quantitative SRM data allowed the 3- and 6-linked Gal isomers to be differentiated. The method was used to relatively quantitate the core 1 glycans from MUC7 to identify any systemic changes in this carbohydrate epitope. A statistically significant increase in sulfation was identified in salivary MUC7 from rheumatoid arthritis patients. This suggests a potential role for this epitope in chronic inflammation. This study was able to develop an SRM approach to specifically identify and relatively quantitate sulfated core 1 isomers and the unsulfated structure. The expansion of this method may afford an avenue for the high throughput investigation of *O*-glycans. *Molecular & Cellular Proteomics 12: 10.1074/mcp.M113.028878, 921–931, 2013.*

From the ‡Department of Medical Biochemistry, Institute of Biomedicine, University of Gothenburg, Medicinaregatan 9A, 405 30, Gothenburg, Sweden, §AB Sciex, Phoenix House, Lakeside Drive, Centre Park, Warrington, WA1 1RX, United Kingdom, and ¶A/B Sciex AB, P. O. Box 1520, 11479, Stockholm, Sweden

Received February 28, 2013
Published, MCP Papers in Press, March 1, 2013, DOI 10.1074/mcp.M113.028878

Glycosylation is a prevalent and significant post-translational modification, exemplified by the existence of a number of congenital and genetic diseases; 64 gene defects have been identified that affect glycan biosynthesis (1). This can result in quite devastating diseases, such as leukocyte-adhesion deficiency type II, which is caused by a loss of sialyl Lewis x production leading to mental retardation, or Wiskott-Aldrich syndrome, which results from problems with *O*-linked glycans in lymphocytes, leading to immunodeficiency (2). Determining specific and global glycan changes is becoming increasingly important, as we gain greater understanding of their significance in health and disease by continuing to improve our tools to investigate them (3).

Glycosylation changes have been observed in many disease states, with several different carbohydrate groups identified as significant. These include carbohydrates from a variety of glycoproteins, including the heavily *O*-glycosylated mucins and mucin-like proteins. Mucins are a group of proteins predominantly found on mucosal surfaces and can be membrane-bound, such as MUC1, MUC4, MUC3A, MUC3B, and MUC16 (also known as CA125), and secreted gel-forming multimeric mucins, including MUC2, MUC5AC, MUC5B, MUC6, MUC19, or monomeric MUC7 (4). Mucin glycosylation is dynamic, and changes have been observed in several types of cancer (5, 6), including testicular germ cell cancer (7), breast cancer (8, 9), and gastric cancer (10). Glycovariants are increasingly being investigated as potential biomarkers such as in pancreatic cancer (11) and immunotherapeutics such as in breast cancer (12).

Although many different *O*-glycans have been associated with disease, it is becoming clear that sulfation of *O*-glycans is critical in many disease states, particularly those of immunological significance. Ulcerative colitis pathogenesis has been associated with an increase in sulfated *O*-glycans (13), and sulfated mucins have also been identified in patients with *Helicobacter pylori* infection (14) and in severe ventilator-associated pneumonia (15).

In this study, *O*-glycosylation changes were addressed in immunological arthritic patients. Arthritis is a large group of

joint conditions, with the most common being rheumatoid arthritis (RA)[1] and osteoarthritis. There are many other forms of arthritis, including the more acute forms such as allergic arthritis and reactive arthritis (ReA). These latter two are generally agreed to be caused by molecular mimicry, resulting in cross-reactive antibodies from gastrointestinal or genitourinary tract bacterial infections, as in ReA, or allergens (16, 17). ReA onset is acute from 1 to 6 weeks post-infection, and usually lasts weeks to months, except for those 30–50% of patients that go on to form a chronic inflammatory response (17). RA is, however, a systemic chronic autoimmune inflammatory disease, affecting 0.5–1% of the world's population. It leads to an altered immune response and hyperproliferation of the synovial lining, causing debilitating joint pain and swelling (18, 19).

Sulfation of *O*-glycans in the synovial tissue and fluid has been suggested to play a role in the pathology of RA, because sulfation was found to be a constituent of the major *O*-glycoprotein, lubricin, found in synovial fluid (SF) from RA patients (20). The level of sulfation correlated with the quantity of rheumatoid factor, indicating a role in chronic state inflammation. However, sulfation has also been indicated to participate in acute phase inflammation, including neutrophil migration (20, 21). Hence, in acute immunological joint conditions like ReA, there may be a different role for sulfation than has been suggested in chronic inflammatory joint disease. The low abundance of these potentially immunologically relevant sulfated oligosaccharides makes them challenging to study.

Mass spectrometry has developed into the most accepted method for analysis of *O*-glycans (22–24). The large scale analysis of *O*-glycans is inhibited by the laborious nature and the expertise required for this analysis, as well as the lack of standards to expedite the annotation process. Furthermore, the need to analyze low abundance glycans requires more sensitive and specific methods and relative quantitation to allow comparison of samples. Selected reaction monitoring (SRM), also known as multiple reaction monitoring, is just such a sensitive and specific quantitative mass spectrometric technique (25, 26). This method uses a triple quadrupole or triple quadrupole/linear ion trap hybrid mass spectrometer (27, 28), where the two mass analyzers are used for filtering. The first quadrupole, Q1, selects the parent mass of interest, which is then fragmented in Q2, and fragment ions analyzed in Q3 for specific ions. Specific transitions are used, *i.e.* pairs of parent and fragment masses that identify an ion of interest, making it highly specific for the target and sensitive due to the reduction in noise. The hybrid mass spectrometer gives the advantage of scanning MS/MS capabilities; this means when an SRM signal satisfies certain threshold criteria, a full scan linear ion trap MS/MS spectrum (enhanced product ion (EPI) spectrum) is triggered of the parent compound. This is referred to as the MIDAS (multiple reaction monitoring initiated detection and sequencing) methodology (29). SRM methodologies are used extensively with small molecules for large scale screening purposes, for example the testing for up to 240 pesticides in food (30) or toxicological analysis of patient samples with several hundred drugs (31, 32). It has also become prevalent in the proteomics field on a large scale (26).

SRM methodologies have been used successfully with glycans, although all have focused on *N*-glycans. Most have used glycopeptides, with methods developed for the quantitation of *N*-glycosylated peptides that have had their glycosylation sites removed (33). Using oxonium ions, which are diagnostic or characteristic ions of glycoproteins, has been effective in identifying and quantifying glycopeptides. Less emphasis has been placed on the identification of specific transitions, instead focusing on compositional information of the identified glycans (34). This approach allows for the general identification of glycopeptides rather than identification of specific ones. A similar method has also been used to analyze variation in *N*-glycan site occupancy in glycopeptides using a standard indicator fragment ion for all glycans (35).

Other methods have focused on specific sugar epitopes. Twenty five SRM transitions for 2-aminopyridine-labeled sialic acid, containing glycopeptides from enriched mouse serum, were successfully created using a fragment ion containing an innermost GlcNAc fragment and quantitatively used to compare normal and diabetic mice (36). A method directed at identification of core-fucosylated proteins has also been developed. Simplified core-fucosylated peptides, containing the fucosyl-GlcNAc glycan, were enriched and used for SRM analysis. This proved to be an effective method, even if unable to differentiate glycoforms (37). Lectins, however, have been used to enrich for various glycosylations associated with disease, before SRM analysis of peptides of interest to analyze glycoforms (38).

Much less work has focused on released glycans; compositional analysis of *N*-glycans has been investigated using a general approach. Compositions of interest were set as the Q1 transition (parent mass) and general *N*-glycan masses for Q3 to identify all *N*-glycans of that mass in a sample (39).

An SRM approach has yet to be developed for *O*-glycans. The highly specific nature of an *O*-glycan SRM approach has the potential to not only allow relative quantitation but also to drastically improve the time-consuming annotation process. Here, the investigation of sulfated core 1 *O*-glycans in acute ReA SF compared with that of chronic RA patients was undertaken. To further investigate the possibility of a systemic sulfation effect and as SF sampling is an invasive technique, sulfation changes in mucin rich- saliva were analyzed. This led to the development of an SRM approach to identify and

[1] The abbreviations used are: RA, rheumatoid arthritis; EPI, enhanced product ion; SRM, selected reaction monitoring; PGC, porous graphitized carbon; PGM, porcine gastric mucin; ReA, reactive arthritis; SDS-AgPAGE, SDS-agarosePAGE; SF, synovial fluid; CE, collision energy; DP, declustering potential; CXP, collision cell exit potential. GalNAcol, *N*-Acetylgalactosaminitol.

relatively quantitate the isomers of the sulfated and unsulfated core 1 *O*-glycans in RA and control salivary MUC7.

EXPERIMENTAL PROCEDURES

Isolation of Acidic Glycoproteins from SF—SF samples from arthritis patients were collected during therapeutic joint aspiration at the Rheumatology Clinic, Sahlgrenska University Hospital (Gothenburg, Sweden). All patients used in this study gave informed consent, and the procedure was approved by the Ethics Committee of the University of Gothenburg. All RA patients fulfilled the American College of Rheumatology 1987 revised criteria for RA (40). The samples were clarified by centrifugation at 10,000 × *g* for 10 min and stored at −80°C before use. The acidic proteins were purified as described previously (41). In brief, the SF sample was diluted with wash buffer (250 mM NaCl, 20 mM Tris-HCl, 10 mM EDTA, pH 7.5) before applying to a 1-ml DEAE-fast flow Hi-Trap column (GE Healthcare). Enriched acidic glycoproteins were eluted with wash buffer containing 1 M NaCl. This fraction was precipitated with 80% ethanol for 16 h at −20°C. The precipitate was collected by centrifugation at 12,100 × *g* for 20 min, air-dried, and then resuspended in PBS. Protein concentration was determined by the BCA protein assay kit (Thermo Scientific, San Jose, CA) using BSA as standard.

The major Alcian blue-staining glycoprotein in the fraction was isolated by SDS-PAGE after reduction by adding 10 mM DTT and heating at 95°C for 20 min and alkylation (25 mM iodoacetamide for 1 h at room temperature) before separation on a 3–8% Tris acetate NuPAGE gel (Invitrogen). Gels were then transferred to PVDF membrane using a semi-dry blotter as described previously (42). Membranes were stained for 20 min using Alcian blue solution (0.125% Alcian blue in methanol with acetic acid) and destained in methanol.

Saliva Samples, AgPAGE Gel Separation, Western Blotting, and Staining—Whole saliva samples were collected from control and RA patients a minimum of 2 h after eating. Saliva was centrifuged at 5000 × *g* for 3 min, and saliva was removed from any remaining pellet.

MUC7 was isolated from whole saliva. The samples were reduced (50 mM DTT, 70°C for 2 h) and alkylated (125 mM iodoacetamide, 30 min at room temperature in the dark) before separation using composite agarose and polyacrylamide (SDS-AgPAGE) gels that were prepared as described previously (42). Each saliva sample was loaded into 4 wells to be sure to account for low abundance of MUC7 in some individuals. Gels were transferred to PVDF and stained with Alcian blue as described for the SF samples, and the lower MUC7 band was excised.

O-Glycan Preparation—*O*-Glycans were released from MUC7 on Alcian blue-stained PVDF membranes by reductive β-elimination. All bands from a single sample were prepared on the same day with the same reagents. Bands were cut from the membrane, and each band was further cut into small squares. Membrane pieces were wet with methanol before the addition of 20 μl of freshly made reductive elimination solution (50 mM sodium hydroxide, 0.5 M sodium borohydride) and incubated at 50°C for 16 h. Samples were neutralized with 1 μl of glacial acetic acid before clean up. Cation exchange columns (AG50WX8 resin, Bio-Rad) were prepared in Ziptips (Millipore, Billerica, MA) using 25 μl of resin suspension (1:1 resin/methanol). Columns were prepared before neutralized samples were washed through, and residual sugar was eluted with water. Samples were dried using a speedvac (45°C) and washed five times with 1% glacial acetic acid in methanol until all borate salts were removed.

Linear Ion Trap Analysis of SF—Porous graphitized carbon (PGC) columns (5-μm particles) were used with an inner diameter of 250 μm and a length of 10 cm packed in-house. Mobile phases consisted of 10 mM ammonium bicarbonate for solvent A and 10 mM ammonium bicarbonate with 80% acetonitrile for solvent B. The gradient, after 5 min of 100% solvent A, increased solvent B to 45% in 41 min and stayed at 100% solvent B for 8 min and then equilibrated at 100% A for 25 min. Columns were attached to an Agilent 1100 series HPLC with a flow rate after passive splitting of 7–10 μl/min. An LTQ linear ion trap (Thermo Fisher Scientific) in negative ion mode was used for MS and MS/MS analysis. A top three data-dependent method was used with normalized collision energy of −35 eV, isolation width of 1.0 *m/z,* and an activation *Q* value of 0.250 and time of 0.250 ms.

SRM Analysis—Mobile phases and PGC columns were used as above with a constant flow of 10 μl/min using an ekspert™ microLC 200 HPLC system (Eksigent, AB Sciex, Framingham, MA). Gradient was as follows: 100% A for 5 min, then a gradient up to 23% B in 21 min, and to 95% B in 5 min. A 20-min wash at 95% was used to keep the column sensitivity high and prevent carry-over, and a 25-min equilibration with 100% A completed the gradient.

SRM analyses were created and carried out on a QTRAP® 5500 ESI-triple quadrupole linear ion trap hybrid mass spectrometer (AB Sciex, Framingham, MA) in negative mode. A ReA lubricin sample was used for creation of the sulfated core 1 *O*-glycan transitions, and *O*-glycans released from porcine gastric mucin (Sigma-Aldrich) were used for the core 1 structure. Optimization of collision energy (CE), declustering potential (DP), and collision cell exit potential (CXP) was performed for each transition tested. The final method for SRM included the following transitions and specifications: 384.1/101.1 (CE −29 eV, DP −25, and CXP −15), 464/241.1 (CE −41 eV, DP −15, and CXP −20), and 464/302.1 (CE −40 eV, DP −15, and CXP −20). A dwell time of 35 ms was used for all. EPI spectra were acquired for the 384 and 464 ions, providing full scan MS/MS data from which sequence analysis could be performed.

Relative Quantitation and Statistical Analysis—MultiQuant™ software version 2.1.1 (AB Sciex, Framingham, MA) was used for semi-quantitation. GraphPad Prism version 5 (GraphPad Software, La Jolla, CA) was used for unpaired two-tailed *t* test statistical analysis.

RESULTS

Identification of Immune-reactive Sulfated Glycans in SF—Glycans have been shown to be essential to a range of immune functions. Here, glycans from the acidic glycoprotein fraction in SF were investigated under either acute or chronic inflammatory conditions to identify specific glycans that were altered. To specifically target *O*-glycans, acidic glycoproteins were isolated from SF using ion exchange chromatography and, following SDS-PAGE separation, transferred to PVDF membrane, and stained with Alcian blue. *O*-Glycans were released from the dominant band by reductive β-elimination and analyzed by LC-MS/MS using PGC chromatography. The pattern of the sulfated core 1 (Galβ1–3GalNAcol) *O*-linked oligosaccharide isomers showed a dramatic difference between the acute and chronic arthritic conditions. It was observed that the patient with the more acute form of arthritic inflammation (ReA) had a more complex pattern of sulfation of core 1 glycans compared with the chronic RA patients. As shown in Fig. 1*A*, the extracted ion chromatograph of the sulfated core 1 with [M − H] of *m/z* 464.1 indicated four different isomers in the ReA patient. The chronic RA patients consistently contained only a single isomer of the sulfated core 1 *O*-glycan at *m/z* 464.1, as shown in the extracted ion chromatograph in Fig. 1*D*.

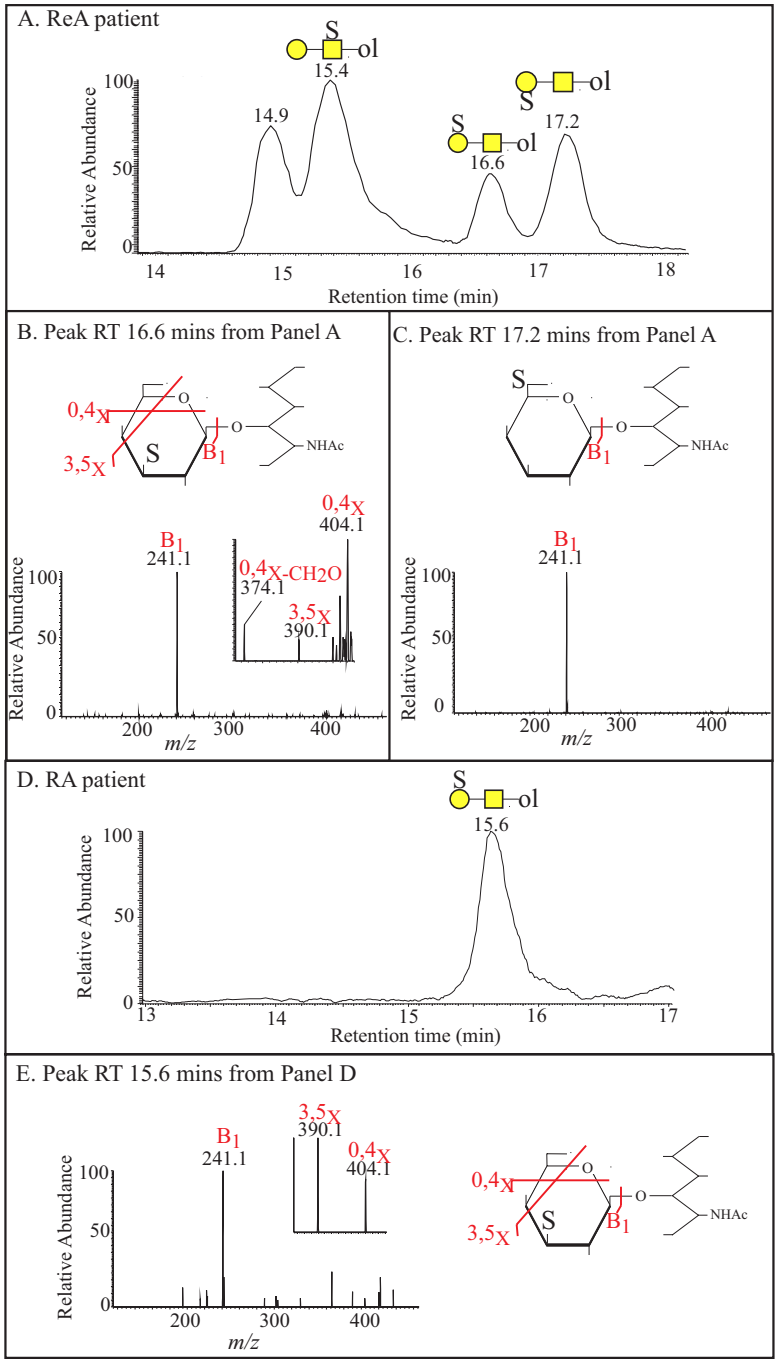

FIG. 1. Extracted ion chromatograph of the sulfated core 1 isomers at *m/z* 464.1 was from the *O*-glycans released from synovial acidic glycoproteins from an ReA patient (*A*) and RA patient (*D*). Three isomers were identified in the ReA patient, one GalNAc-linked (RT 15.4 min) and two Gal-linked (RTs 16.6 and 17.2 min). A single Gal-linked isomer was identified in the RA patient (RT 15.6 min). The MS/MS (using a linear ion trap) from the two Gal-linked isomers from the ReA patient (*A*) are shown in *B* and *C*. The 3-linked sulfated isomer is shown (*B*) with the site-indicative cross-ring fragments and the 6-linked in *C*. The MS/MS (using a linear ion trap) of the Gal-linked isomer from the RA patient (*D*) is shown in *E* with the cross-ring fragments indicating a 3-linked sulfate. *Yellow square* represents GalNAc; *yellow circle* is Gal, and *S* indicates sulfate.

Investigation of the Type of Sulfation of Core 1 Isomers, Differentiating Gal-linked Sulfate Isomers—MS/MS spectra of the sulfated core 1 isomers were analyzed to determine the location of the sulfate group on the disaccharide. The four isomeric *O*-glycans released from the acidic synovial glycoproteins from the ReA (Fig. 1*A*) sample produced MS/MS spectra indicating that the location of the sulfate was on either the Gal or the GalNAcol residue. For three of these, the location of the sulfate could be assigned to either of the residues by detection of diagnostic fragment ions in the MS/MS spectra. However, the first peak (RT 14.9 min) showed a MS/MS spectrum indicating a mixed sulfate position between the two-residue isomers. This may be due to sulfate migration, which has been shown to occur during MS/MS fragmentation under certain conditions (43). Because the biological significance of this mixed isomer was not clear and the sulfate could not be assigned, further work focused on the structures that could be assigned by MS/MS.

The second chromatographic peak (Fig. 1*A*) with RT 15.4 min was identified as having the sulfate group attached to the

GalNAcol moiety (intense Y ion of *m/z* 302 and Z ion of *m/z* 284) (this spectrum not reproduced here as it is consistent with the spectra shown in Fig. 4*A*, see under "Development of an SRM Method for Relative Quantification of Sulfated and Unsulfated Core 1 O-Linked Glycans"). Both 3- and 6-linked sulfation has been recorded for sulfation of the reducing end GalNAc; however, because the 3-position was occupied by the Gal residue, the component most likely consists of the 6-linked sulfate linked to GalNAc. The third (RT 16.6 min) and fourth (RT 17.2 min) components in the chromatogram were both characterized as isomers where sulfate is linked to the Gal moiety (Fig. 1, *B* and *C*). When observing the MS/MS of these isomers, the *m/z* 241 fragment, consisting of the sulfated Gal B type ion, dominated the spectra, in effect dampening the rest of the spectrum. Despite this, it was possible to observe low intensity fragments that revealed the location of the sulfate in the *S*-Gal isomer that eluted at RT 16.6 min (Fig. 1*B*). The ^{0,4}X (*m/z* 404.1) and ^{3,5}X (*m/z* 390.1) fragments together with a ^{0,4}X-CH_2O (*m/z* 374.1) fragment were found to be exclusive to this isomer, as they were not found in the later-eluting sulfate-Gal isomer eluted at RT 17.2 min (Fig. 1*C*). These site-indicative cross-ring fragments designate either the 2nd or 3rd carbon of the Gal to be sulfated. Biologically, sulfate has been described as attached to the 3rd and 6th carbon of Gal. Hence, it can be surmised that the peak at RT 16.6 min is the 3-linked isomer. This then also implied that the other Gal-linked isomer with RT 17.2 min (Fig. 1*C*) was the 6-linked isomer.

Analysis of the MS/MS of the single sulfated core 1 *O*-glycan isomer (RT 15.6 min, Fig. 1*D*) identified in the chronic RA patients was also undertaken. Fragmentation spectra showed that the sulfate was linked to Gal, determined by the prominent *m/z* 241.1 fragment (Fig. 1*E*). The position of the sulfate on the Gal was also able to be determined as the 3-linked isomer due to presence of cross-ring fragments as described above.

Comparison of Salivary and SF O-Linked Oligosaccharides, Identification of Sulfation of Core-1 O-Glycan in Saliva—Given the identification of the sulfated core 1 *O*-glycans as an immune-reactive epitope at the site of inflammation, these glycans were investigated further. RA is a chronic systemic inflammatory disease, and the possibility that the sulfated core 1 epitopes are also immunologically reactive at a systemic level was considered. The noninvasive sampling of saliva (a rich source of *O*-linked mucin glycoproteins) was deemed suitable for analyzing systemic sulfation. Therefore, the *O*-glycans released from salivary MUC7 were compared with those from the major acidic glycoprotein of SF to ascertain if this is an appropriate sample.

Whole saliva samples were separated by SDS-AgPAGE, as was described for the SF glycoproteins. The Alcian blue-stained PVDF membranes for SF and saliva are shown in Fig. 2, *A* and *C*, respectively. Although the SF sample had a distinct major band, the saliva sample shows a higher molecular weight MUC5B and lower MUC7 band. After excising the appropriate MUC7 band, *O*-glycans were released by reductive β-elimination and analyzed by LC-MS/MS using PGC chromatography (Fig. 2, *B* and *D*).

The difference between SF glycosylation and saliva glycosylation is illustrated by the level of complexity of the released oligosaccharide detected. LC-MS of oligosaccharides from a representative (ReA) SF sample (Fig. 2*B*) was dominated by core 1 structures (Galβ1–3GalNAcol) with and without the extension of sialic acid as identified previously in SF glycoproteins (41). The most intense [M − H] ion of *m/z* 675.2 corresponds to the monosialylated core 1 structure NeuAcα2–3Galβ1–3GalNAcol, and the prominent but less intense [M − H] ions of *m/z* 966.3 and *m/z* 384.1 correspond to the disialylated (NeuAcα2–3Galβ1–3(NeuAcα2–6)GalNAcol) and nonsialylated (Galβ1–3GalNAcol) core 1 structures, respectively. Further investigation of low abundance oligosaccharides identified the sulfated core 1 structure with an [M − H] ion at *m/z* 464.1 (Fig. 2*A, inset*). In comparison, MUC7 (Fig. 2*D*) was found to have a more diverse and abundant *O*-glycosylation profile, including more complex oligosaccharides as described previously (44). Fewer core 1 structures were observed as shown in Fig. 2*D*. The most abundant peak, like the SF sample, was the monosialylated core 1 structure NeuAcα2–3Galβ1–3GalNAcol with an [M − H] ion of *m/z* 675.2. The sulfated core 1 structure with an [M − H] ion at *m/z* 464.1 and unsulfated core 1 structure with an [M − H] ion of *m/z* 384.1 were both identified in low abundance, although in some saliva samples, these structures were below the level of detection by full scan LC-MS using a linear ion trap.

The identification of the sulfated core 1 *O*-glycan on MUC7 confirmed this glycoprotein as an appropriate sample to investigate the systemic importance of this epitope in chronic inflammation. However, the abundance of this and the unsulfated precursor was low and inconsistently detected between patients because of the limit of detection of the full scan LC-MS approach used. A more specific and sensitive approach was needed to further this research; hence, a targeted SRM approach was developed to address the issue of systemic core 1 sulfation.

Development of an SRM Method for Relative Quantification of Sulfated and Unsulfated Core 1 O-Linked Glycans—To further investigate core 1 sulfated isomers in salivary MUC7, a more sensitive and semiquantitative SRM method was developed for these low abundance glycans. The method aimed to determine the relative proportion of the sulfated core 1 structure in relation to its unsulfated core 1 biosynthetic precursor, as well as being able to distinguish the sulfate isomer as either S-Gal or S-GalNAc. Ideally, the method would also differentiate the two possible *S*-Gal isomers.

SRM method development was made more difficult by the lack of appropriate commercially available *O*-glycan standards. However, the *O*-glycans released from ReA SF glycoprotein containing all possible sulfated isomers, along with the

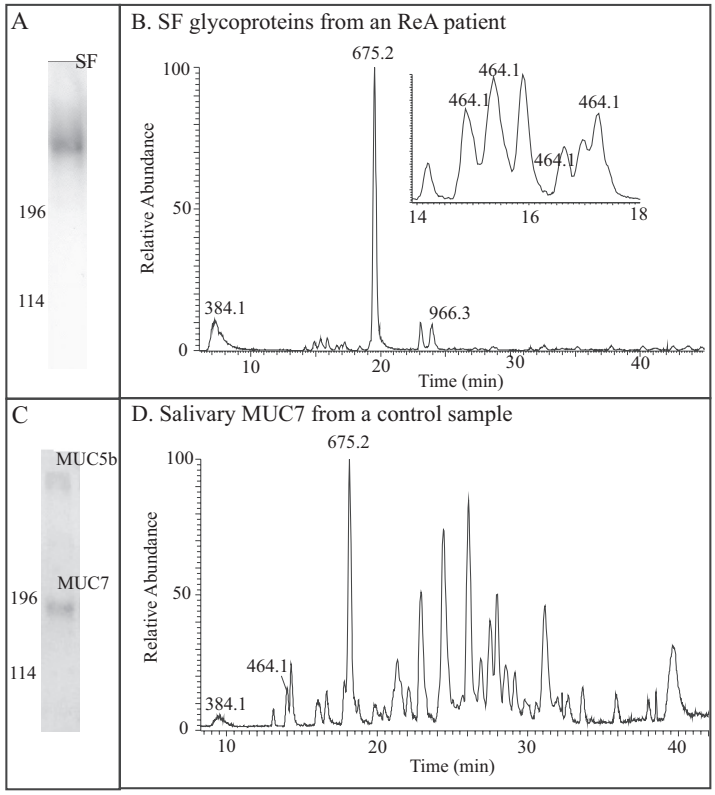

FIG. 2. **Comparison of Alcian blue-stained PVDF membranes after SDS-AgPAGE separation and base peak chromatographs from the *O*-glycans, which were then released by reductive β-elimination of an enriched SF sample from a ReA patient (*A* and *B*) and salivary MUC7 from a control sample (*C* and *D*).** Core 1 structures are indicated on the base peak with [M − H] ions for the core 1 *O*-glycan of *m/z* 384.1, sulfated core 1 of m/z 464.1, sialylated core 1 of *m/z* 675.2, and disialylated core 1 of *m/z* 966.3. The ReA sample shows a major band (*A*), and when *O*-glycans were released, the sample showed an abundance of core 1 structures, with the lower abundance sulfated core 1 structure inlaid (*B*). The saliva sample shows a higher molecular weight MUC5B and lower molecular weight MUC7 band (*C*). *O*-Glycans were released, and the base peak is shown in *D*. The base peak is more complex than the SF (*B*) with a single sulfated core 1 peak.

O-glycans released from PGM for the unsulfated core 1 *O*-glycan, provided an appropriate although complex sample. This complexity necessitated the need for the optimization to be performed on the column.

The unsulfated core 1 precursor at *m/z* 384 required little CE for fragmentation in the QTRAP® hybrid instrument, as observed in Fig. 3*A* where a CE of −23 eV was used, resulting in numerous strong fragments as candidates for use in an SRM transition. It was, however, found that the fragmentation of this small *O*-glycan was variable. This variability is illustrated in Fig. 3*B*. The eight most prominent MS/MS fragments were chosen and the intensities compared for 50 randomly selected scans. The range of relative intensities for the fragments is observed. The fragments at *m/z* 89, 222, and 229 had a low median and were often not apparent, and although the fragments at *m/z* 126, 138, and 156 had a higher median and high relative intensities in many scans, they were still absent in some scans. The Z-type fragment at *m/z* 204 was consistently the most intense fragment. This is the mass of a GalNAcol in negative ion mode making it a ubiquitous fragment in *O*-glycans, also observed in the sulfated isomers (see Fig. 4). This suggests specificity rather than sensitivity could be an issue, particularly if this method was extended to larger *O*-glycans in the future. The second most intense fragment of *m/z* 101 was therefore chosen as it was consistently observed in the unsulfated core 1 MS/MS spectra and was not observed in the sulfated isomers. The stability of this ion was further optimized for use in the SRM method.

During the optimization process, it was observed that the fragmentation of the sulfated core 1 disaccharides resulted in few highly dominating fragments (Fig. 4), similar to that observed in the linear ion trap (Fig. 1). The MS/MS fragmentation patterns of the sulfated isomers were distinct from each other as well as from the unsulfated glycan (Fig. 3). For each of the *S*-Gal and *S*-GalNAc isomers, the most prominent peaks were the monosaccharide with the sulfate attached, making an ideal, specific, and intense SRM transition. The *S*-GalNAc isomer (Fig. 4*A*) had both the Z (*m/z* 284.1) and Y (*m/z* 302.1) fragments, and the two *S*-Gal-linked isomers (Fig. 4, *B* and *C*) both have only the B fragment (*m/z* 241.1). The increase in CE between the sulfated glycans (−40 eV) and unsulfated glycan (−23 eV) was much greater than anticipated by mass increase alone, suggesting interestingly that the sulfate may increase the stability of this small *O*-glycan.

EPI spectra were used to differentiate the two *S*-Gal isomers, as differentiation was possible in the MS/MS fragmentation spectra acquired in the linear ion trap. This method acquires fragmentation spectra for all compounds that meet the SRM criteria. The MS/MS spectra acquired in the QTRAP® instrument for the two *S*-Gal isomers were able to differentiate between the isomers, despite the prominence of the dominating *m/z* 241.1 fragment. The *S*-Gal isomer eluting first (RT 9.8 min) had the $^{3,5}X$ (*m/z* 390.1) and $^{0,4}X$ (*m/z* 404.1) cross-ring fragments (Fig. 4*B*) indicating the 3-linked sulfate isomer, consistent with the ion trap data. These identifying cross-ring fragments were low in relative abundance; however, the low

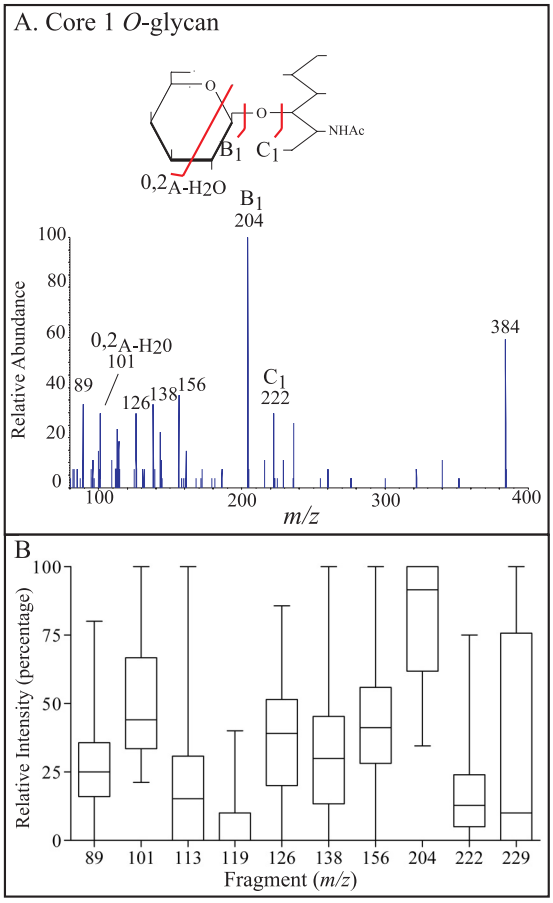

FIG. 3. *A*, MS/MS of the unsulfated core 1 *O*-glycan with an [M − H] ion at *m/z* 384.1 fragmented in the QTRAP® ESI-triple quadrupole linear ion trap hybrid mass spectrometer. *B,* relative intensities of the 10 most intense fragments were collected for 50 MS/MS scans at the standard CE of −35 eV. A boxplot presents these data. A large variation was observed in the relative intensities for the fragments shown by the broad boxes indicating the median and lower first and upper third quartiles. The large ranges for the fragments are shown by the maximum and minimum.

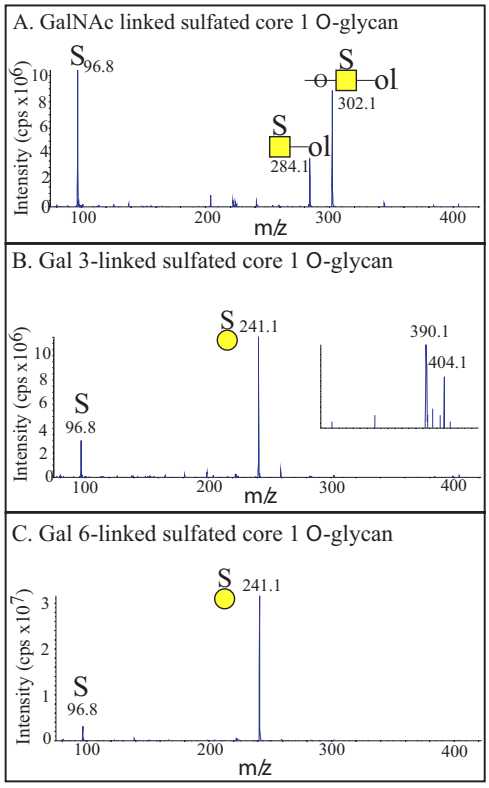

FIG. 4. **MS/MS fragmentation of the three possible sulfated isomers with [M − H] of *m/z* 464.1 in the QTRAP® ESI triple-quadrupole linear ion trap hybrid mass spectrometer used for SRM analysis.** The glycosidic fragments used in SRM transitions are indicated. The GalNAc-linked sulfate isomer is shown in *A* and the two possible Gal-linked isomers, the 3-linked Gal isomer (*B*) showing site indicative cross-ring fragments (inlaid) and the 6-linked Gal isomer (*C*). *Yellow square* represents GalNAc; *yellow circle* is Gal, and *S* indicates sulfate.

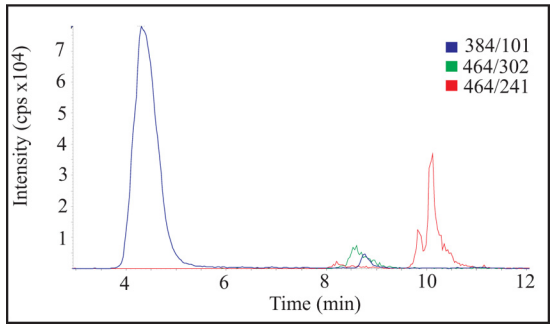

FIG. 5. **SRM trace of the final SRM method using the ReA SF and PGM released *O*-glycans that were used for SRM method development.** The three transitions are observed. The 384/101 transition (indicating the unsulfated core 1 structure) is shown in *blue*. The 464/302 transition (indicating the GalNAc-linked sulfate isomer) is shown in *green*. The 464/241 transition (indicating the Gal-linked sulfate isomers) is displayed in *red* showing two peaks for the two isomers. The faster gradient for the SRM as described under "Experimental Procedures" was used for the experiments.

background given in the SRM method and the identification of these fragments even at low sample concentrations provide confidence in this approach. This indicates the *S*-Gal isomer eluting later (RT 10.1 min) was the 6-linked sulfate isomer.

The final SRM method contained three transitions as follows: the unsulfated core 1 (384.1/101.1), *S*-Gal isomer (464.1/241.1), and *S*-GalNAc isomer (464.1/302.1). The use of EPI spectra, giving the MS/MS fragmentation information, along with retention time, allowed the differentiation of the two Gal-linked isomers. The three transitions are shown in Fig. 5, which is the mixture of the biological standards used for optimization (synovial glycoprotein and PGM).

Relative Quantitation of Systemic Core 1 Sulfation in RA Patients—To investigate the role of sulfation in inflammation, control and RA patient saliva were compared using the SRM method developed in this study. MUC7 was isolated by SDS-AgPAGE and transferred to PVDF membrane for reductive β-elimination. Following SRM analysis, the area under the curve was calculated for both the 384 and 464 isomers. The MultiQuant program was found to be the most appropriate

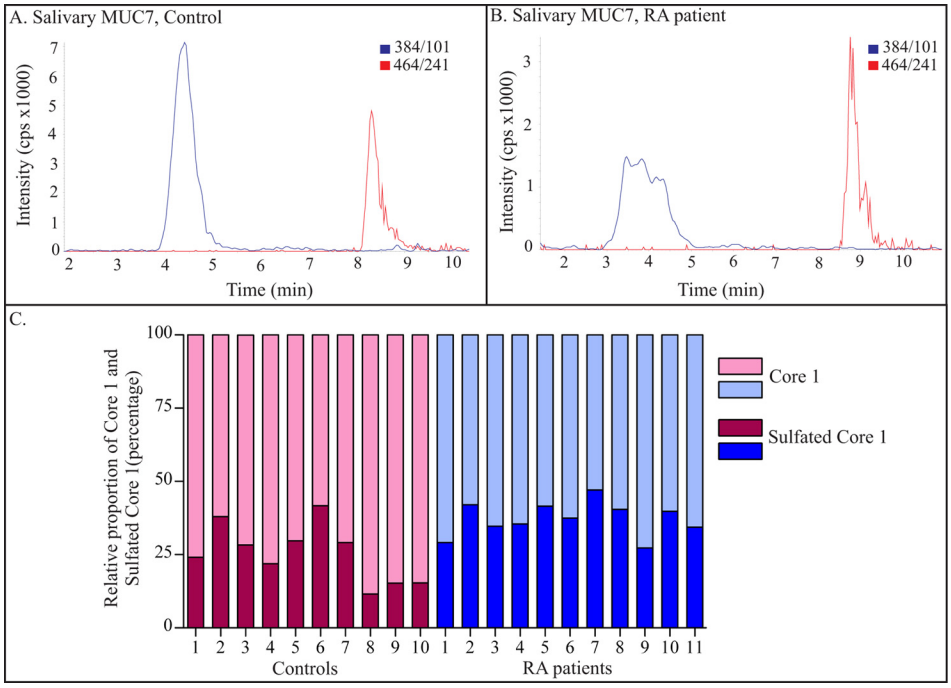

FIG. 6. ***O*-Glycans were released by reductive β-elimination from the salivary MUC7 of 10 control and 11 RA patients after separation of whole saliva by SDS-AgPAGE.** SRM traces of the control (*A*) and RA patients (*B*) show the 384/101 transition (indicating the unsulfated core 1 structure) is shown in *blue,* and 464/241 transition (indicating the Gal-linked isomer) is shown in *red*. The single Gal-linked isomer was shown to be the 3-linked sulfate in all samples. The SRM method was used to relatively quantitate the proportion of sulfated core 1 *O*-glycan compared with the unsulfated core 1 *O*-glycan. The data are shown graphically (*C*) as the percentage of sulfated and unsulfated core 1 *O*-glycan in each sample. A two-tailed *t* test showed a statistically significant difference (*p* value 0.0055), with an increase in sulfation in the RA patients. The faster gradient for the SRM as described under "Experimental Procedures" was used for the experiments.

program for selecting the broad and jagged peaks seen with the PGC chromatography of these small *O*-glycans. This automation reduced the need for manual peak selection, reducing the time and variability when analyzing large data sets.

In all control and RA patients (see Fig. 6*A*), there was only a single isomer of the sulfated 464 structure with the sulfate attached to the Gal, transition 464.1/241.1. This isomer, as well as the unsulfated structure, was present in all 10 control and all the 11 RA samples. The MS/MS spectra obtained using the full scan linear ion trap MS/MS spectra enabled the identification of the sulfated isomer as the 3-Gal-linked isomer (as in Fig. 3*B*), as was observed in the RA synovial sample, suggesting the core 1 3-Gal-linked isomer is consistent in chronic inflammation.

The relative proportion of sulfated compared with unsulfated core 1 *O*-glycans was ascertained and the data shown in Fig. 6*B* as a percentage of sulfated *versus* unsulfated. In all samples, there was a higher proportion of the unsulfated core 1 structure compared with the 3-Gal-sulfated core 1 isomer detected in the salivary MUC7 of control and RA patients. When comparing the relative quantities between controls ($n = 10$) and RA patients ($n = 11$), it was found on average (mean ± S.E.) that there was 25.5% (±1.75) sulfated core 1 *O*-glycan in the controls and 37.2% (± 3.11) in the RA patients. When comparing the control and RA patients using an unpaired two-tailed *t* test, there was a statistically significant difference (*p* value of 0.0055). Hence, we demonstrate that in this small sample set there is a statistically significant increase in core 1 sulfation in the salivary MUC7 of RA patients compared with normal controls. This may suggest that core 1 *O*-glycan sulfation is not only reactive to the immunological conditions at the site of inflammation but also at a systemic level.

DISCUSSION

Development of an SRM Method for Core 1 O-Glycans—The large scale analysis of glycans is hindered by the time-consuming nature and expertise necessary for analysis. This is due to the lack of resources for automatic interpretation making manual annotation necessary. Here, the need for a more sensitive method was also apparent, and an SRM method for sulfated and unsulfated core 1 *O*-glycans was successfully developed. Current glycan SRM methods have focused solely on *N*-glycans. These studies have investigated the detection of total *N*-glycans (34, 35), compositional analysis (39), or identification of specific traits (38), rather than annotation or structural elucidation of individual glycans. The work described here concentrated on *O*-glycans, and a more specific approach was attempted to distinguish isomeric structures.

Chromatographic separation of glycan isomers is essential for the complete investigation of an *O*-glycan sample, especially as our understanding of the importance of specific isomers continues to develop. PGC chromatography has been used for almost 2 decades in conjunction with mass spectrometry (45), and it has become a robust method for separation of both *N*- and *O*-glycans, particularly due to its ability to separate isomers (46). PGC was able to show that the number and type of sulfated core 1 isomers were distinctly different between the acute ReA and chronic RA samples of released glycans from synovial glycoproteins (see Fig. 1). It was used here to aid in distinguishing glycan isomers in this SRM method.

The core 1 structure showed some variability when fragmented with changes in the relative abundance of each fragment between MS/MS spectra as represented in Fig. 3. The impact of this variation was reduced given the large number of available MS/MS fragments. The two most consistent fragments were the glycosidic Z fragment at *m/z* 204 and the cross-ring fragment *m/z* 101. The Z fragment was the most intense and has been used in other methods that aim to identify total glycans, as the fragment is ubiquitous in glycan analysis (35). However, this study aimed to develop a method to provide specific structural information, not only glycan identification. For this reason, the cross-ring fragment was chosen because of its greater specificity as it is rarely observed in larger core 1 structures (Fig. 4). This would also be an advantage should the method be expanded to include larger core 1 structures that may undergo degradation and disrupt semi-quantitative analysis. The more specific, slightly less intense fragment was considered the most appropriate choice for this method.

The aims of the developed SRM method were first to identify and distinguish the sulfated and unsulfated core 1 structures and second to successfully differentiate the Gal and GalNAc sulfated isomers. The linear ion trap used for the initial investigation (Fig. 1) and QTRAP® instrument (Figs. 3 and 4) used for SRM analyses gave very similar fragmentation patterns for the sulfated structures studied. In both instruments, the glycosidic fragments were dominant, providing optimal specific and intense transitions for distinguishing the isomers. The ability of the QTRAP® instrument to acquire highly sensitive full scan linear ion trap MS/MS spectra, in addition to quantitative SRM data, allowed more specific annotation of the two possible *S*-Gal isomers. The site-specific ^{3,5}X and ^{0,4}X cross-ring fragments (Fig. 4, *A* and *B*) allowed the distinction of the 3-linked isomer from the 6-linked isomer (Fig. 4). The time required for analysis as well as the amount of sample necessary are reduced by performing both EPI and SRM analysis in a single run, a unique feature of the QTRAP® instrument. It also allowed the SRM method developed here to distinguish the unsulfated and all three possible sulfated isomers of the core 1 structure.

The success of this method has opened the possibility of expansion into a much larger range of *O*-glycans. The development of *O*-glycan resources, such as Unicarb-DB, will aid in this process (47). Unicarb-DB is an LC-MS database of published glycan data. It includes HPLC and MS data and methods, including MS/MS spectra, as well as annotation where available, which has the potential to significantly increase the ease of developing SRM experiments. This is especially significant given the lack of commercially available *O*-glycans for method development. Although development of *O*-glycan SRM methods is challenging, the ease of data analysis makes it an ideal approach to make *O*-glycan analysis more accessible and make high throughput analysis possible.

Investigation of Sulfation in Inflammatory Disease—A difference in the sulfated core 1 isomers in acute and chronic arthritic inflammation was observed in the *O*-glycans released from synovial glycoproteins at the site of inflammation. An increase in sulfated core 1 isomers was observed in the SF in acute arthritis at the site of inflammation. The acute ReA *O*-glycans contained all possible isomers of the sulfated core 1 *O*-glycan with the sulfate on the GalNAc and on both the 3- and 6-positions of the Gal (Fig. 1). An additional peak was also observed; however, this was unable to be identified as a single isomer, and its biological significance is currently undeterminable, particularly given it was not identified by further SRM analyses. This range of sulfated isomers was not observed in the chronic RA samples. A single isomer, the 3-Gal isomer, was observed in all RA patients.

The presence of the 6-linked isomers, either to Gal or GalNAc, in acute inflammation and not in chronic inflammation indicates a role for these epitopes in the acute phase. This suggests that the sulfotransferases that add 6-linked sulfate to Gal and GalNAc are active in the acute and not active in chronic inflammation. This is consistent with the suggestion that that there is one sulfotransferase that can act on both these sites and is active in acute inflammation (8). These data suggest that sulfated glycans are important at the site of inflammation, and isomers are regulated to the specific stage of inflammation to which they are necessary.

RA is a complicated immunological disease, and sulfotransferases and sulfated glycans have been indicated as important to specific disease processes. RA begins with an acute innate inflammatory response. This involves the antigen-presenting cells as follows: dendritic cells, macrophages, and activated B cells presenting arthritis-associated antigens to T cells. T cells pass through the synovium membrane via high endothelial venules (48, 49). These high endothelial venules have been shown to up-regulate a specific sulfotransferase, GlcNAc6ST-2 (50); however, this enzyme is not responsible for the sulfation seen here. This up-regulation is due to the importance of this epitope for lymphocyte homing where sialyl Lewis x and other similar core 2 glycans with sialic acid, core fucosylation, and sulfation have been shown to bind the lymphocyte L-selectin (51). There has been no evidence that core

1 structures can be involved in lymphocyte homing; however, it has been suggested in previous studies on synovial *O*-glycans that a conformational grouping of important epitopes are effective in L-selectin binding (41), in which the isomers seen here may be involved.

The identification of these glycan epitopes as reactive to the immediate immunological conditions led to the investigation of this glycan at a systemic level under chronic inflammatory conditions. Salivary MUC7 was investigated as an appropriate sample to investigate core 1 sulfation changes in RA. The total *O*-glycans were compared with those from the SF acidic glycoproteins (Fig. 2). The Gal 3-linked sulfate core 1 structure was identified in MUC7 along with the unsulfated form, although in very low abundance (Fig. 2). The development of the SRM method negated the concern of low abundance due to its increased sensitivity, making this an appropriate sample for analysis of sulfation at a systemic level.

The SRM method was used to relatively quantitate the proportion of sulfated compared with unsulfated core 1 *O*-glycans in RA and control salivary MUC7. This allowed the investigation into a possible shift in the level of sulfation during systemic inflammation. The SRM method was also able to show a statistically significant difference with a relative increase in the sulfated structure compared with the unsulfated in saliva from RA patients. This suggests a possible systemic up-regulation of this structure specifically, or sulfated structures in general, in chronic systemic inflammation; however the small sample size makes it difficult to determine the biological significance of this finding.

In RA there is a shift to chronic inflammation, and there remains an increase in T cells compared with healthy joint tissue. There is also B cell differentiation and autoantibody production leading to the destruction observed in RA patients (48, 49). This study suggests that it is at this point that up-regulation of 3-linked sulfated core 1 occurs. Previous work has indicated that nonfucosylated sulfated glycans may be specific to joint inflammation (41); however, the possibility of systemic up-regulation of this small sulfated glycan suggests that this sulfated epitope, or sulfate in general, may have a role in systemic inflammation. Whether this role is related to the cause or the result of systemic inflammation and whether it is specific to this glycan epitope requires further investigation.

Concluding Remarks—Here, a streamlined SRM workflow was presented to allow high throughput sample analysis to differentiate and relatively quantitate sulfated isomers and unsulfated core 1 *O*-glycan structures from salivary MUC7 samples. The specificity of this approach aids in the annotation of these structures, greatly reducing the time needed for data analysis of *O*-glycans. This method could be extended to include other *O*-glycans and make the large scale high throughput analysis of *O*-glycans more accessible and realistic. This method was then applied successfully to identify systemic changes in *O*-glycosylation on salivary MUC7 during the chronic inflammatory disease rheumatoid arthritis. This result suggests an as yet unidentified role for core 1 *O*-glycan sulfation in chronic systemic inflammation.

Acknowledgments—We are grateful to Prof. Ulf Dahlgren and Christina Eklund from the Department of Odontology, University of Gothenburg, for providing us with the patient samples. Anna-Karin Hultgård Ekwall, Lena Björkman, and Maria Bokarewa from the Department of Rheumatology and Inflammation Research, University of Gothenburg, kindly provided patient SF samples. The LTQ mass spectrometer was obtained by Grant 342-2004-4434 from the Swedish Research Council.

* This work was supported by the Swedish Research Council Grant 621-2010-5322 and The Swedish Foundation for International Cooperation in Research and Higher Education.

‖ To whom correspondence should be addressed. Tel.: 46-31-7866528; Fax: 46-31-416108; E-mail: niclas.karlsson@medkem.gu.se.

REFERENCES

1. Hennet, T. (2012) Diseases of glycosylation beyond classical congenital disorders of glycosylation. *Biochim. Biophys. Acta* **1820,** 1306–1317
2. Durand, G., and Seta, N. (2000) Protein glycosylation and diseases: blood and urinary oligosaccharides as markers for diagnosis and therapeutic monitoring. *Clin. Chem.* **46,** 795–805
3. Hart, G. W., and Copeland, R. J. (2010) Glycomics hits the big time. *Cell* **143,** 672–676
4. McGuckin, M. A., Lindén, S. K., Sutton, P., and Florin, T. H. (2011) Mucin dynamics and enteric pathogens. *Nat. Rev. Microbiol.* **9,** 265–278
5. Hollingsworth, M. A., and Swanson, B. J. (2004) Mucins in cancer: protection and control of the cell surface. *Nat. Rev. Cancer* **4,** 45–60
6. Hakomori, S. (2002) Glycosylation defining cancer malignancy: new wine in an old bottle. *Proc. Natl. Acad. Sci. U.S.A.* **99,** 10231–10233
7. Rajpert-De Meyts, E., Poll, S. N., Goukasian, I., Jeanneau, C., Herlihy, A. S., Bennett, E. P., Skakkebaek, N. E., Clausen, H., Giwercman, A., and Mandel, U. (2007) Changes in the profile of simple mucin-type *O*-glycans and polypeptide GalNAc transferases in human testis and testicular neoplasms are associated with germ cell maturation and tumour differentiation. *Virchows Archiv.* **451,** 805–814
8. Seko, A., Ohkura, T., Ideo, H., and Yamashita, K. (2012) Novel *O*-linked glycans containing 6′-sulfo-Gal/GalNAc of MUC1 secreted from human breast cancer YMB-S cells: possible carbohydrate epitopes of KL-6(MUC1) monoclonal antibody. *Glycobiology* **22,** 181–195
9. Ghosh, S. K., Pantazopoulos, P., Medarova, Z., and Moore, A. (2012) Expression of underglycosylated MUC1 antigen in cancerous and adjacent normal breast tissues. *Clin. Breast Cancer* **13,** 109–118
10. Conze, T., Carvalho, A. S., Landegren, U., Almeida, R., Reis, C. A., David, L., and Söderberg, O. (2010) MUC2 mucin is a major carrier of the cancer-associated sialyl-Tn antigen in intestinal metaplasia and gastric carcinomas. *Glycobiology* **20,** 199–206
11. Haab, B. B., Porter, A., Yue, T., Li, L., Scheiman, J., Anderson, M. A., Barnes, D., Schmidt, C. M., Feng, Z., and Simeone, D. M. (2010) Glycosylation variants of mucins and CEACAMs as candidate biomarkers for the diagnosis of pancreatic cystic neoplasms. *Ann. Surg.* **251,** 937–945
12. Lavrsen, K., Madsen, C. B., Rasch, M. G., Woetmann, A., Odum, N., Mandel, U., Clausen, H., Pedersen, A. E., and Wandall, H. H. (2012) Aberrantly glycosylated MUC1 is expressed on the surface of breast cancer cells and a target for antibody-dependent cell-mediated cytotoxicity. *Glycoconj. J.* DOI 10.1007/s10719-012-9437-7
13. Kobayashi, M., Fukuda, M., and Nakayama, J. (2009) Role of sulfated *O*-glycans expressed by high endothelial venule-like vessels in pathogenesis of chronic inflammatory gastrointestinal diseases. *Biol. Pharm. Bull.* **32,** 774–779
14. Cohen, M. C., Rúa, E. C., Balcarce, N., and Drut, R. (2000) Sulfomucins in *Helicobacter pylori*-associated chronic gastritis in children: is this incipient intestinal metaplasia? *J. Pediatr. Gastroenterol. Nutr.* **31,** 63–67
15. Dennesen, P., Veerman, E., van Nieuw Amerongen, A., Jacobs, J., Kessels, A., van der Keybus, P., Ramsay, G., and van der Ven, A. (2003) High levels of sulfated mucins in bronchoalveolar lavage fluid of ICU patients

with ventilator-associated pneumonia. *Intensive Care Med.* **29,** 715–719
16. Morris, D., and Inman, R. D. (2012) Reactive arthritis: developments and challenges in diagnosis and treatment. *Curr. Rheumatol. Rep.* **14,** 390–394
17. Carter, J. D. (2010) Treating reactive arthritis: insights for the clinician. *Ther. Adv. Musculoskelet. Dis.* **2,** 45–54
18. Firestein, G. S. (2003) Evolving concepts of rheumatoid arthritis. *Nature* **423,** 356–361
19. Gay, S., Gay, R. E., and Koopman, W. J. (1993) Molecular and cellular mechanisms of joint destruction in rheumatoid arthritis: two cellular mechanisms explain joint destruction? *Ann. Rheum. Dis.* **52,** S39–S47
20. Jin, C., Ekwall, A. K., Bylund, J., Björkman, L., Estrella, R. P., Whitelock, J. M., Eisler, T., Bokarewa, M., and Karlsson, N. G. (2012) Human synovial lubricin expresses sialyl Lewis x determinant and has L-selectin ligand activity. *J. Biol. Chem.* **287,** 35922–35933
21. Subramanian, H., Grailer, J. J., Ohlrich, K. C., Rymaszewski, A. L., Loppnow, J. J., Kodera, M., Conway, R. M., and Steeber, D. A. (2012) Signaling through L-selectin mediates enhanced chemotaxis of lymphocyte subsets to secondary lymphoid tissue chemokine. *J. Immunol.* **188,** 3223–3236
22. Jensen, P. H., Kolarich, D., and Packer, N. H. (2010) Mucin-type *O*-glycosylation–putting the pieces together. *FEBS J.* **277,** 81–94
23. North, S. J., Hitchen, P. G., Haslam, S. M., and Dell, A. (2009) Mass spectrometry in the analysis of *N*-linked and *O*-linked glycans. *Curr. Opin. Struct. Biol.* **19,** 498–506
24. Schulz, B. L., Packer, N. H., and Karlsson, N. G. (2002) Small-scale analysis of *O*-linked oligosaccharides from glycoproteins and mucins separated by gel electrophoresis. *Anal. Chem.* **74,** 6088–6097
25. Boja, E. S., and Rodriguez, H. (2012) Mass spectrometry-based targeted quantitative proteomics: achieving sensitive and reproducible detection of proteins. *Proteomics* **12,** 1093–1110
26. Picotti, P., and Aebersold, R. (2012) Selected reaction monitoring-based proteomics: workflows, potential, pitfalls, and future directions. *Nat. Methods* **9,** 555–566
27. Le Blanc, J. C., Hager, J. W., Ilisiu, A. M., Hunter, C., Zhong, F., and Chu, I. (2003) Unique scanning capabilities of a new hybrid linear ion trap mass spectrometer (Q TRAP) used for high sensitivity proteomics applications. *Proteomics* **3,** 859–869
28. Hager, J. W., and Yves Le Blanc, J. C. (2003) Product ion scanning using a Q-q-Q linear ion trap (Q TRAP) mass spectrometer. *Rapid Commun. Mass Spectrom.* **17,** 1056–1064
29. Anderson, L., and Hunter, C. L. (2006) Quantitative mass spectrometric multiple reaction monitoring assays for major plasma proteins. *Mol. Cell. Proteomics* **5,** 573–588
30. Zhang, K., Wong, J. W., Yang, P., Hayward, D. G., Sakuma, T., Zou, Y., Schreiber, A., Borton, C., Nguyen, T. V., Kaushik, B., and Oulkar, D. (2012) Protocol for an electrospray ionization tandem mass spectral product ion library: development and application for identification of 240 pesticides in foods. *Anal. Chem.* **84,** 5677–5684
31. Dresen, S., Ferreirós, N., Gnann, H., Zimmermann, R., and Weinmann, W. (2010) Detection and identification of 700 drugs by multitarget screening with a 3200 Q TRAP LC-MS/MS system and library searching. *Anal. Bioanal. Chem.* **396,** 2425–2434
32. Wissenbach, D. K., Meyer, M. R., Weber, A. A., Remane, D., Ewald, A. H., Peters, F. T., and Maurer, H. H. (2012) Toward a universal LC-MS screening procedure, can an LIT LC-MS(*n*) screening approach and reference library be used on a quadrupole-LIT hybrid instrument? *J. Mass Spectrom.* **47,** 66–71
33. Kim, Y. J., Zaidi-Ainouch, Z., Gallien, S., and Domon, B. (2012) Mass spectrometry-based detection and quantification of plasma glycoproteins using selective reaction monitoring. *Nat. Protoc.* **7,** 859–871
34. Song, E., Pyreddy, S., and Mechref, Y. (2012) Quantification of glycopeptides by multiple reaction monitoring liquid chromatography/tandem mass spectrometry. *Rapid Commun. Mass Spectrom.* **26,** 1941–1954
35. Gil, G. C., Velander, W. H., and Van Cott, K. E. (2009) *N*-Glycosylation microheterogeneity and site occupancy of an Asn-*X*-Cys sequon in plasma-derived and recombinant protein C. *Proteomics* **9,** 2555–2567
36. Kurogochi, M., Matsushista, T., Amano, M., Furukawa, J., Shinohara, Y., Aoshima, M., and Nishimura, S. (2010) Sialic acid-focused quantitative mouse serum glycoproteomics by multiple reaction monitoring assay. *Mol. Cell. Proteomics* **9,** 2354–2368
37. Zhao, Y., Jia, W., Wang, J., Ying, W., Zhang, Y., and Qian, X. (2011) Fragmentation and site-specific quantification of core-fucosylated glycoprotein by multiple reaction monitoring-mass spectrometry. *Anal. Chem.* **83,** 8802–8809
38. Ahn, Y. H., Lee, J. Y., Lee, J. Y., Kim, Y. S., Ko, J. H., and Yoo, J. S. (2009) Quantitative analysis of an aberrant glycoform of TIMP1 from colon cancer serum by L-PHA-enrichment and SISCAPA with SRM mass spectrometry. *J. Proteome Res.* **8,** 4216–4224
39. Zhang, H., Wang, Z., Stupak, J., Ghribi, O., Geiger, J. D., Liu, Q. Y., and Li, J. (2012) Targeted glycomics by selected reaction monitoring for highly sensitive glycan compositional analysis. *Proteomics* **12,** 2510–2522
40. Arnett, F. C., Edworthy, S. M., Bloch, D. A., McShane, D. J., Fries, J. F., Cooper, N. S., Healey, L. A., Kaplan, S. R., Liang, M. H., Luthra, H. S., *et al*. (1988) The American Rheumatism Association 1987 revised criteria for the classification of rheumatoid arthritis. *Arthritis Rheum.* **31,** 315–324
41. Estrella, R. P., Whitelock, J. M., Packer, N. H., and Karlsson, N. G. (2010) The glycosylation of human synovial lubricin: implications for its role in inflammation. *Biochem. J.* **429,** 359–367
42. Hayes, C. A., Nemes, S., Issa, S., Jin, C., and Karlsson, N. G. (2012) Glycomic work-flow for analysis of mucin *O*-linked oligosaccharides. *Methods Mol. Biol.* **842,** 141–163
43. Kenny, D. T., Issa, S., and Karlsson, N. G. (2011) Sulfate migration in oligosaccharides induced by negative ion mode ion trap collision-induced dissociation. *Rapid Commun. Mass Spectrom.* **25,** 2611–2618
44. Karlsson, N. G., and Thomsson, K. A. (2009) Salivary MUC7 is a major carrier of blood group I type *O*-linked oligosaccharides serving as the scaffold for sialyl Lewis x. *Glycobiology* **19,** 288–300
45. Davies, M. J., Smith, K. D., Carruthers, R. A., Chai, W., Lawson, A. W., and Hounsell, E. F. (1993) Use of a porous graphitised carbon column for the high-performance liquid chromatography of oligosaccharides, alditols, and glycopeptides with subsequent mass spectrometry analysis. *J. Chromatogr. A* **646,** 317–326
46. Jensen, P. H., Karlsson, N. G., Kolarich, D., and Packer, N. H. (2012) Structural analysis of *N*- and *O*-glycans released from glycoproteins. *Nat. Protoc.* **7,** 1299–1310
47. Hayes, C. A., Karlsson, N. G., Struwe, W. B., Lisacek, F., Rudd, P. M., Packer, N. H., and Campbell, M. P. (2011) UniCarb-DB: a database resource for glycomic discovery. *Bioinformatics* **27,** 1343–1344
48. Nakken, B., Munthe, L. A., Konttinen, Y. T., Sandberg, A. K., Szekanecz, Z., Alex, P., and Szodoray, P. (2011) B-cells and their targeting in rheumatoid arthritis–current concepts and future perspectives. *Autoimmun. Rev.* **11,** 28–34
49. Choy, E. (2012) Understanding the dynamics: pathways involved in the pathogenesis of rheumatoid arthritis. *Rheumatology* **51,** Suppl. 5, v3–11
50. Pablos, J. L., Santiago, B., Tsay, D., Singer, M. S., Palao, G., Galindo, M., and Rosen, S. D. (2005) A HEV-restricted sulfotransferase is expressed in rheumatoid arthritis synovium and is induced by lymphotoxin-α/β and TNF-α in cultured endothelial cells. *BMC Immunol.* **6,** 6
51. McEver, R. P. (2005) A sulfated address for lymphocyte homing. *Nat. Immunol.* **6,** 1067–1069